Expression, purification and crystallization of a dye-decolourizing peroxidase from *Dictyostelium discoideum*

Amrita Rai, Roman Fedorov and Dietmar J. Manstein
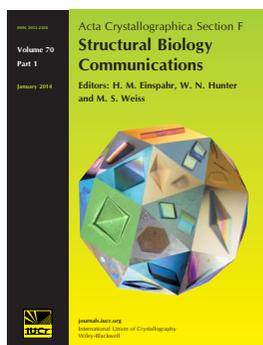
Acta Crystallographica Section F: Structural Biology Communications is a rapid all-electronic journal, which provides a home for short communications on the crystallization and structure of biological macromolecules. Structures determined through structural genomics initiatives or from iterative studies such as those used in the pharmaceutical industry are particularly welcomed. Articles are available online when ready, making publication as fast as possible, and include unlimited free colour illustrations, movies and other enhancements. The editorial process is completely electronic with respect to deposition, submission, refereeing and publication.

Crystallography Journals Online is available from **journals.iucr.org**

Expression, purification and crystallization of a dye-decolourizing peroxidase from *Dictyostelium discoideum*

Amrita Rai, Roman Fedorov and Dietmar J. Manstein*

Institute for Biophysical Chemistry, Medizinische Hochschule Hannover, Carl-Neuberg-Strasse 1, 30625 Hannover, Germany

Correspondence e-mail: manstein.dietmar@mh-hannover.de

Dye-decolourizing peroxidases are haem-containing peroxidases with broad substrate specificity. Using H_2O_2 as an electron acceptor, they efficiently decolourize various dyes that are of industrial and environmental relevance, such as anthraquninone- and azo-based dyes. In this study, the dye-decolourizing peroxidase DdDyP from *Dictyostelium discoideum* was overexpressed in *Escherichia coli* strain Rosetta(DE3)pLysS, purified and crystallized using the vapour-diffusion method. A native crystal diffracted to 1.65 Å resolution and belonged to space group $P4_12_12$, with unit-cell parameters $a = b = 141.03$, $c = 95.56$ Å, $\alpha = \beta = \gamma = 90°$. The asymmetric unit contains two molecules.

1. Introduction

Dye-decolourizing peroxidases (DyPs) are a relatively recently recognized superfamily of haem-containing peroxidases (Kim & Shoda, 1999). They are present in a wide range of fungi and bacteria. Phylogenetically, DyPs are divided into four subfamilies (A–D). The members of subfamilies A–C are mostly of bacterial origin, whereas subfamily D mostly consists of fungal DyPs (Ogola *et al.*, 2009). Depending on the substrate, DyPs display pH optima in the range 2–5. DyPs are of industrial interest as they are able to degrade a wide range of complex organic molecules. They enzymatically oxidize high-redox-potential anthraquninone dyes (Sugano *et al.*, 2006). Moreover, some DyPs show peroxidase activity towards nonphenolic lignin model compounds. They efficiently turn over methoxylated aromatics such as veratryl alcohol and more common peroxide substrates such as 2,20-azinobis(3-ethylbenzthiazoline-6-sulfonic acid) (ABTS; Ogola *et al.*, 2009). DypB from *Rhodococcus jostii* RHA1 has been shown to oxidize Mn^{2+} (Roberts *et al.*, 2011).

The catalytic mechanism of DyPs is similar to that of plant-type peroxidases (Sugano, 2009). The resting ferric enzyme reacts with H_2O_2 to yield Compound I, an Fe^{4+} oxoferryl centre and a porphyrin-based cation radical $[Fe^{IV}{=}O\ Por^{\bullet}]^+$. Compound I reacts with one equivalent of the reducing substrate to yield another intermediate, Compound II $[Fe^{IV}{=}O]$. Further addition of a second equivalent of the reducing substrate yields the resting-state Fe^{III} peroxidase. Nevertheless, structural studies of DyPs indicate differences from plant peroxidases (Zubieta, Krishna *et al.*, 2007; Sugano *et al.*, 2007). They have a ferredoxin-like fold, similar to that of chlorite dismutase (de Geus *et al.*, 2009). In both plant peroxidases and DyPs the haem group is ligated by a proximal histidine, whereas the residues on the distal face of the haem are different. DyPs have a conserved aspartate and arginine on the distal face, while a catalytic histidine is present in the plant peroxidases (Zubieta, Krishna *et al.*, 2007; Sugano *et al.*, 2007). Several recent studies have pointed out the major differences between the catalytic mechanisms of DyP peroxidases and other peroxidases. Based on the structure of fungal DyPs, it has been proposed that the aspartate of the G*XX*DG motif swings into the proper position required for interaction with H_2O_2, leading to the formation of Compound I (Yoshida *et al.*, 2011). However, analysis of the peroxidative cycle of DypB from *R. jostii* RHA1 shows that a conserved DypB arginine is essential for peroxidase activity, while the replacement of aspartate by alanine has only a marginal effect on the reactivity towards H_2O_2 and the formation of Compound I (Singh *et al.*, 2012).
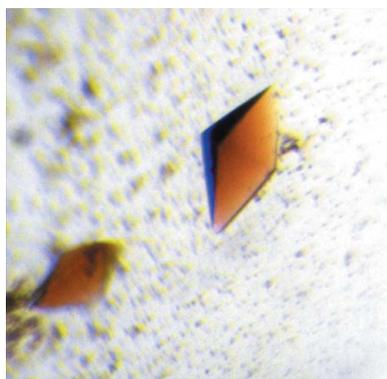
Table 1
Diffraction data-collection and processing statistics for *Dictyostelium* DdDyP.

Values in parentheses are for the outer resolution shell.

Beamline	ID29, ESRF Grenoble
Detector	Pilatus 6M
Wavelength (Å)	0.91985
Crystal-to-detector distance (mm)	313.233
Exposure time per image (s)	0.0375
No. of images	1200
Oscillation range (°)	0.3
Space group	$P4_12_12$
Unit-cell parameters (Å, °)	$a = b = 141.03$, $c = 95.56$, $\alpha = \beta = \gamma = 90$
Crystal mosaicity (°)	0.13
No. of molecules in asymmetric unit	2
Resolution range (Å)	47.78–1.65 (1.75–1.65)
No. of total/unique reflections	3073816/115557
Completeness (%)	100.00 (100.0)
Multiplicity	26.6 (26.5)
Mean $I/\sigma(I)$	17.0 (2.3)
R_{merge} (%)	3.2 (44.9)
$CC_{1/2}$†	99.9 (73.8)

† Percentage of correlation between intensities from random half data sets.

To date, only two eukaryotic DyP proteins have been structurally characterized, both of fungal origin. To investigate the catalytic mechanism and structure–function relationship of eukaryotic DyPs, structural and mechanistic studies involving enzymes from other phyla are required. Unlike fungal DyPs, *Dictyostelium* DyP is not secreted and is only present in cytoplasm. It shares characteristics with prokaryotic and fungal DyPs as well as with horseradish-type peroxidases. Moreover, initial characterization showed distinct spectral properties for the reaction intermediates. Here, we report the cloning, expression, purification, crystallization and preliminary X-ray crystallographic analysis of the first DyP from *D. discoideum*.

2. Materials and methods

2.1. Plasmid construction and overexpression of recombinant *Dictyostelium* DdDyP

The gene encoding dye-decolourizing peroxidase was amplified from *Dictyostelium* genomic DNA (GenBank accession No. XM_639419.1) by PCR. For the PCR reaction, we used a forward primer which contains a *Bam*HI site (bold) followed by specific nucleotides of the 5′ DdDyP gene (GATC**GGATCC**ATGGCACAGTCAACAGTGTTACCAATGCAT) and a reverse primer specific for the 3′ sequence including a stop codon followed by an *Xho*I site (bold) (GATC**CTCGAG**TTACAATTCTAATAATTCTTTTTTTGATGG). The PCR product was cloned into the plasmid PGEX 6P1-4CS (Tzvetkov *et al.*, 2006). The construct was verified by sequencing and the plasmid was transformed into *Escherichia coli* Rosetta (DE3)pLysS.

2.2. Expression and purification

Transformed *E. coli* Rosetta(DE3)pLysS cells were grown in Luria–Bertani medium containing 100 µg ml^{-1} ampicillin and 34 µg ml^{-1} chloramphenicol. Cells were grown at 310 K until the $OD_{600 nm}$ reached ∼1.0. Protein expression was induced by the addition of 1 mM isopropyl β-D-1-thiogalactopyranoside (IPTG) for 16 h at 290 K. The cells were harvested by centrifugation (4000g) and washed with PBS. Prior to purification, the pellets were stored at 193 K.

For purification, the cell pellets were thawed and resuspended in lysis buffer (50 mM Tris pH 8.0, 150 mM NaCl) supplemented with an EDTA-free protease-inhibitor cocktail (Roche). Lysis was started by the addition of 0.5 mg ml^{-1} lysozyme and 0.1%(v/v) Triton X-100 followed by 5 min sonication at 30% maximum intensity in a Branson 250 sonicator. Cell debris was removed by centrifugation at 21 000g for 45 min. The resulting supernatant was loaded onto a Glutathione Sepharose column pre-equilibrated with lysis buffer. After extensive washing with lysis buffer, the protein was cleaved on the column by PreScission protease at a molar ratio of 500:1. Cleaved protein was eluted by lysis buffer. Purified preparations of *Dictyostelium* DdDyP had R_z values (Abs$_{Soret}$/Abs$_{280}$) of <0.1, indicating the absence of a haem group. To reconstitute the protein, haemin chloride dissolved in DMSO was added dropwise with gentle stirring to a final 2:1 haemin:protein molar ratio. Excess haemin chloride was removed *via* centrifugation followed by gel-filtration chromatography using a HiLoad 26/60 Superdex 200 prep-grade column (GE Healthcare) equilibrated with lysis buffer. The flow rate was adjusted to 1 ml min^{-1}. Peak fractions were pooled and concentrated to 10 mg ml^{-1} using an ultrafiltration system (Vivaspin 10K, Sartorius Stedim Biotech). The protein concentration was determined using the Bio-Rad protein assay reagent with BSA as a standard. The purity of the protein was confirmed by SDS–PAGE. The absorption spectrum of 10 µM DdDyP was recorded using a Shimadzu UV-2700 UV–Vis spectrophotometer at room temperature. Reconstituted DdDyP gave an R_z value of 2.0. Protein supplemented with 3%(w/v) sucrose was flash-frozen in liquid N$_2$ and stored at 193 K.

2.3. Crystallization

Initial crystallization screening was performed at 293 K by the sitting-drop vapour-diffusion method using commercial crystallization screens (Qiagen), 96-well Intelli-Plates and a Phoenix robot (Art Robbins Instruments). Each crystallization drop was prepared by mixing 0.25 µl reservoir solution and 0.25 µl protein solution, and the mixture was equilibrated against 0.1 ml reservoir solution. After one week, crystals appeared in 2.4 M sodium malonate pH 7.0. We refined the crystallization condition at 293 K by the hanging-drop vapour-diffusion method using 24-well plates (Linbro, MP Biomedicals). 2 µl protein solution was mixed with 2 µl reservoir solution and equilibrated against 700 µl reservoir solution; conditions were further optimized by varying the protein and precipitant concentrations as well as the pH of the sodium malonate solution.

2.4. Data collection and X-ray diffraction analysis

Diffraction data were collected from DdDyP crystals at a wavelength of 0.91985 Å at 100 K on beamline ID29 at the European Synchrotron Radiation Facility (ESRF), Grenoble, France equipped with a Pilatus 6M pixel detector (Dectris). Single crystals were transferred to cryoprotectant solution [reservoir solution + 15%(v/v) glycerol] and then flash-cooled directly in liquid nitrogen. A complete data set was collected to 1.65 Å resolution. The oscillation angle was 0.3°. The diffraction data were indexed, integrated and scaled with the *XDS* software package (Kabsch, 2010). Data-collection and processing statistics are given in Table 1.

2.5. Preliminary structure analysis

Molecular-replacement calculations were performed using the *Phaser* module (McCoy *et al.*, 2007) in the *CCP*4 software suite (Winn *et al.*, 2011). Self-rotation function analysis was performed using the *AMoRe* module (Navaza, 2001) in *CCP*4.

crystallization communications

3. Results and discussion

Full-length DdDyP (molecular weight 34.9 kDa) was successfully overexpressed in *E. coli* Rosetta(DE3)pLysS cells and purified to homogeneity using a glutathione affinity column and subsequent size-exclusion chromatography (Fig. 1*a*). The absorption spectrum of ferric DdDyP showed distinct spectral features. DdDyP has a Soret band at 400 nm and charge-transfer bands, CT1 and CT2, at 638 and 506 nm; the R_z value of DdDyP corresponds to 2.0 (Fig. 1*b*). Initial screening of the crystallization conditions was performed by the sitting-drop vapour-diffusion method using 1248 commercially available unique crystallization conditions (Qiagen). DdDyP crystals were optimized using the hanging-drop vapour-diffusion method. The best quality crystals grew after two weeks at 293 K in a 4 μl hanging drop consisting of a 1:1 mixture of protein solution (10 mg ml⁻¹) and 2.4 *M* sodium malonate pH 7.0. The crystals grew with a tetragonal bipyramidal shape. A single crystal was used for data collection (Fig. 2). The native DdDyP crystal diffracted to 1.65 Å resolution on synchrotron beamline ID29 at the ESRF, Grenoble, France (Fig. 3). A full 360° data set was collected using a crystal-to-detector distance of 313.233 mm with 0.3° oscillation and 0.0375 s exposure per image. Processing of the X-ray diffraction data indicates that the native DdDyP crystal belonged to space group $P4_12_12$, with unit-cell para-

meters $a = b = 141.03$, $c = 95.56$ Å, $\alpha = \beta = \gamma = 90°$. The Matthews coefficient calculated using the cell-content analysis program showed that there are two or three molecules in the asymmetric unit; two molecules give a V_M value of 3.4 Å³ Da⁻¹ and 63.8% solvent content, whereas three molecules give a V_M value of 2.3 Å³ Da⁻¹ with 45.7% solvent content (Matthews, 1968).

We are currently in the process of solving the structure of DdDyP using the molecular-replacement method with the structure of *Shewanella oneidensis* TyrA (PDB entry 2iiz; Zubieta, Joseph *et al.*, 2007) as the search model. DdDyP exhibits 37% sequence identity to *Shewanella* TyrA. The molecular-replacement procedure using the TyrA structure as an initial model resulted in clear solutions for both the rotation and the translation functions corresponding to a dimer in the asymmetric unit, which belongs to space group $P4_12_12$. A translation-function search using the enantiomorphic space group
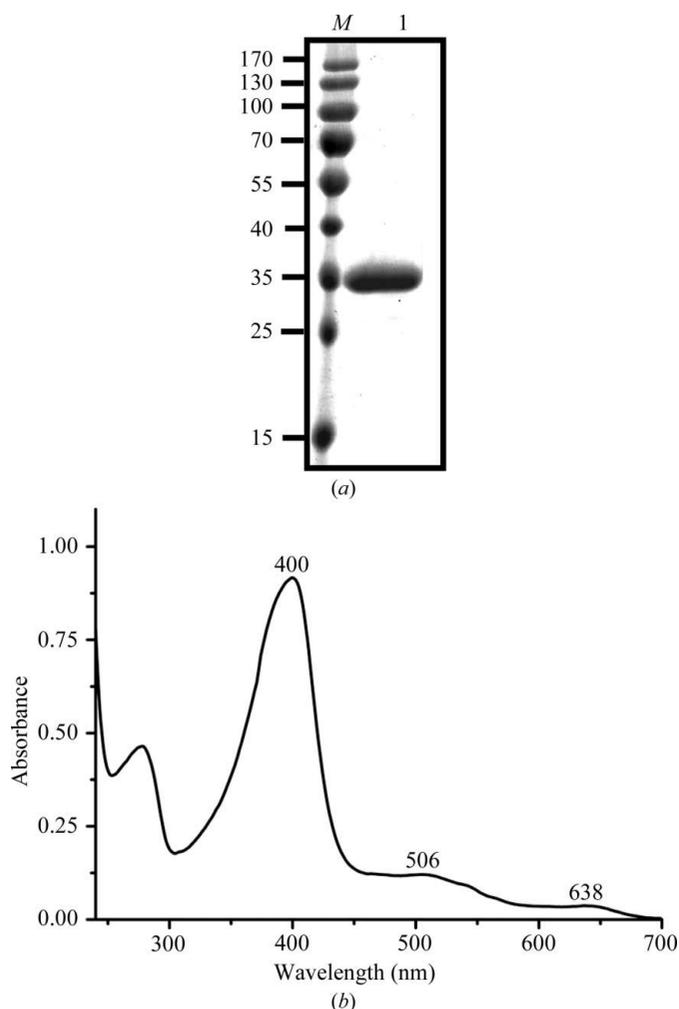

Figure 2
Crystal of DdDyP (average dimensions of $200 \times 100 \times 50$ μm).

Figure 1
Recombinant *Dictyostelium* DdDyP. (*a*) SDS–PAGE of DdDyP protein stained with Coomassie Blue. Lane *M*, molecular-weight markers (labelled in kDa); lane 1, 10 μg DdDyP protein. (*b*) Electronic absorption spectrum of 10 μ*M* DdDyP in lysis buffer.
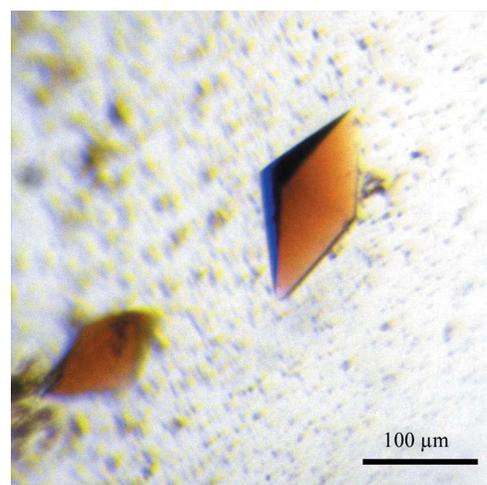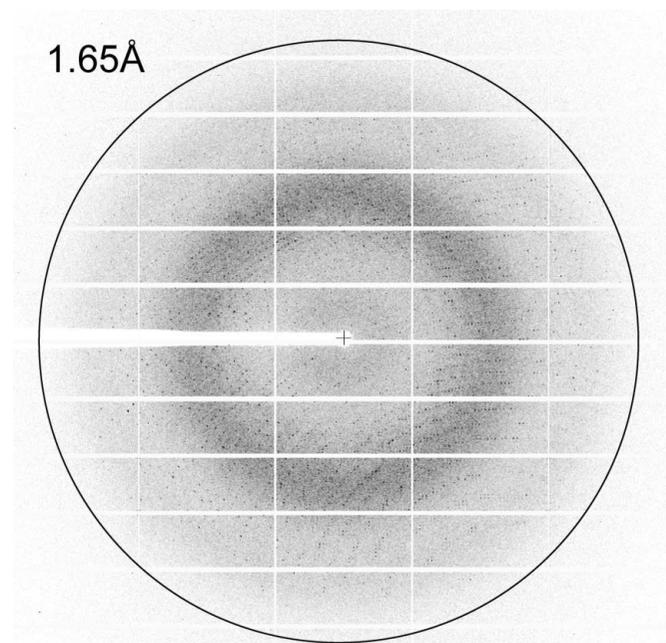

Figure 3
X-ray diffraction image of DdDyP. The circle is at 1.65 Å resolution.

$P4_32_12$ resulted in much lower correlation values and a loss of contrast between the translation-function solutions. No additional molecules were found in the asymmetric unit, the electron-density maps were of high quality and no clashes were found between molecules. The dimeric state of DdDyP in the asymmetric unit is also supported by analysis of the self-rotation function (see §2 for details). The initial R-factor and R_{free} values resulting from the molecular-replacement solution were 43.5 and 49.5%, respectively. After the first round of simulated annealing (*CNS*) followed by a minimization procedure, the R factor and R_{free} fell to 32.3 and 34.4%, respectively (Brünger *et al.*, 1998). Crystal-packing and electron-density analysis revealed a high solvent content in the crystal, which may explain the relatively high value observed for the Matthews coefficient (3.4 $\text{Å}^3\,\text{Da}^{-1}$). Model-building and refinement procedures are in progress.

In parallel with structural studies, kinetic measurements are being carried out with the wild type as well as with mutants of important distal residues in the peroxidative cycle in order to shed light on the catalytic mechanism and substrate specificity of *Dictyostelium* DdDyP. The final structural details and the results of kinetic measurements will be described in a separate paper.

References

Brünger, A. T., Adams, P. D., Clore, G. M., DeLano, W. L., Gros, P., Grosse-Kunstleve, R. W., Jiang, J.-S., Kuszewski, J., Nilges, M., Pannu, N. S., Read, R. J., Rice, L. M., Simonson, T. & Warren, G. L. (1998). *Acta Cryst.* D**54**, 905–921.
Geus, D. C. de, Thomassen, E. A., Hagedoorn, P. L., Pannu, N. S., van Duijn, E. & Abrahams, J. P. (2009). *J. Mol. Biol.* **387**, 192–206.
Kabsch, W. (2010). *Acta Cryst.* D**66**, 125–132.
Kim, S. J. & Shoda, M. (1999). *Appl. Environ. Microbiol.* **65**, 1029–1035.
Matthews, B. W. (1968). *J. Mol. Biol.* **33**, 491–497.
McCoy, A. J., Grosse-Kunstleve, R. W., Adams, P. D., Winn, M. D., Storoni, L. C. & Read, R. J. (2007). *J. Appl. Cryst.* **40**, 658–674.
Navaza, J. (2001). *Acta Cryst.* D**57**, 1367–1372.
Ogola, H. J., Kamiike, T., Hashimoto, N., Ashida, H., Ishikawa, T., Shibata, H. & Sawa, Y. (2009). *Appl. Environ. Microbiol.* **75**, 7509–7518.
Roberts, J. N., Singh, R., Grigg, J. C., Murphy, M. E., Bugg, T. D. & Eltis, L. D. (2011). *Biochemistry*, **50**, 5108–5119.
Singh, R., Grigg, J. C., Armstrong, Z., Murphy, M. E. & Eltis, L. D. (2012). *J. Biol. Chem.* **287**, 10623–10630.
Sugano, Y. (2009). *Cell. Mol. Life Sci.* **66**, 1387–1403.
Sugano, Y., Matsushima, Y. & Shoda, M. (2006). *Appl. Microbiol. Biotechnol.* **73**, 862–871.
Sugano, Y., Muramatsu, R., Ichiyanagi, A., Sato, T. & Shoda, M. (2007). *J. Biol. Chem.* **282**, 36652–36658.
Tzvetkov, N., Breuer, P. & Boteva, R. (2006). *Biotechniques*, **40**, 145–146.
Winn, M. D. *et al.* (2011). *Acta Cryst.* D**67**, 235–242.
Yoshida, T., Tsuge, H., Konno, H., Hisabori, T. & Sugano, Y. (2011). *FEBS J.* **278**, 2387–2394.
Zubieta, C., Joseph, R. *et al.* (2007). *Proteins*, **69**, 234–243.
Zubieta, C., Krishna, S. S. *et al.* (2007). *Proteins*, **69**, 223–233.